

Uncertainties in estimating water fluxes and residence times using environmental tracers in an arid unsaturated zone

Bridget R. Scanlon

Bureau of Economic Geology, University of Texas at Austin

Abstract. Environmental tracers are used widely to evaluate flow processes and estimate fluxes and ages of pore water in arid regions. The purpose of this study was to evaluate uncertainties in water flux and age on the basis of data from environmental tracers, including meteoric Cl, ^{36}Cl , ^3H , $\delta^2\text{H}$, and $\delta^{18}\text{O}$ in porous media. Representative profiles of environmental tracers from drainage and interdrainage areas at a site in the Chihuahuan Desert of Texas were evaluated. The chloride mass balance approach (CMB) was used to evaluate water fluxes and ages. The long residence times indicated by the Cl data in interdrainage areas (55,000 to 105,000 years to 25 m depth) were generally corroborated by residence times estimated from radioactive decay of ^{36}Cl ($39,000 \pm 13,000$ to $59,000 \pm 14,400$ years). Uncertainties in the CMB approach include uncertainties in transport processes, Cl input, and Cl output. Although the CMB approach assumes one-dimensional, downward piston flow, water potential and stable isotope data in interdrainage areas suggest net upward water movement. Cl data indicate that drying of the profiles may have persisted throughout the Holocene ($\sim 10,000$ years). Therefore the downward flow assumption may only be applicable in the older, deeper sections of the profiles. Cl diffusion is significant near the surface where Cl concentration gradients are steep. Anion exclusion may affect calculated water fluxes based on Cl in clay-rich zones. Although it is difficult to quantify uncertainties in diffusion and anion exclusion processes, they act in concert and result in overestimation of water flux and underestimation of age by the CMB approach. Therefore, in interdrainage areas the CMB approach provides an upper bound on actual water fluxes and a lower bound on actual ages. Error bars on these bounding estimates were evaluated on the basis of uncertainties in Cl input ($\sim \pm 35\%$) and in Cl output ($\pm 3\%$) that result in $\pm 38\%$ uncertainty in water flux and -24 to 56% uncertainty in water age in interdrainage areas. In drainage areas it is much more difficult to apply the CMB approach because of preferential flow, large uncertainties in Cl input as a result of run-on, reduced sensitivity of Cl to water flux, and analytical uncertainties in Cl measurements. Although preferential flow was shown by ^3H data, mixing calculations suggest that $^{36}\text{Cl}/\text{Cl}$ ratios cannot be used to evaluate preferential flow when Cl concentrations in the matrix exceed 10 to 100 g m^{-3} , as is found in the playa and the fissure. Neglecting Cl input from run-on results in underestimation of water flux by about an order of magnitude. Therefore the apparent CMB water flux, which ignores preferential flow and run-on, represents a lower bound on the actual water flux in contrast to an upper bound for interdrainage areas. These results have important implications for waste disposal in arid regions because they suggest that water fluxes estimated using the CMB approach are conservatively high in interdrainage areas characterized by porous media.

1. Introduction

Interest in water flux through thick, unsaturated zones in arid regions has increased greatly in the last couple of decades because of concerns about waste disposal, including proposed low-level and high-level radioactive waste disposal sites in the United States, and groundwater contamination, such as at the Hanford Reservation in Washington, Sandia National Laboratory in New Mexico, and other sites. With increased development of arid regions, water-resource concerns have also become important, and recharge to the underlying aquifers has become critical to maintaining current and proposed development in these regions.

Copyright 2000 by the American Geophysical Union.

Paper number 1999WR900240.
0043-1397/00/1999WR900240\$09.00

Many techniques for quantifying long-term net water fluxes and residence times or ages of pore water in arid systems rely on environmental tracers [Allison *et al.*, 1994; Phillips, 1994]. There are, however, various sources of uncertainty related to estimating water fluxes and ages from tracer data. Evaluation of water fluxes and ages from tracer data is an inverse process that involves inferring or assuming the tracer input and transport processes required to produce the measured tracer output. Tracer output, which corresponds to the subsurface distribution of tracers, is generally measured. Uncertainties related to analytical measurements of tracer-output concentrations are readily evaluated. Such uncertainties generally reflect the precision of laboratory measurements and not accuracy, which is determined by how well calibrated an instrument is with respect to some absolute or defined standard. The measured tracer concentration is assumed to represent the average

in situ concentration of the infiltrating water at the sampled depth. Uncertainties associated with tracer input are generally more difficult to quantify. The validity of estimated transport processes will also result in uncertainties in estimated water fluxes and ages. In some cases, more than one conceptual model can result in the same tracer distribution, and we have to rely on corroborative evidence from other tracers or physical data to discriminate between different models and resolve non-unique problems.

The chloride mass balance (CMB) approach has been used in many studies to quantify water fluxes and ages [Allison and Hughes, 1978]. Water flux in the unsaturated zone can be estimated from the degree of Cl enrichment in pore water as a result of evapotranspiration relative to the Cl concentration in precipitation. Uncertainties associated with the CMB approach include uncertainties in the Cl input to the system, in transport processes, and in Cl output or Cl concentrations measured in pore water. Applications of the CMB approach assume that the transport process is approximated by one-dimensional (1-D), downward piston flow. Although the CMB approach assumes downward water movement, water-potential measurements in interdrainage areas of many basins in the southwestern United States indicate that the driving force for water movement is upward in the top 20 to 40 m [Scanlon *et al.*, 1997b]. In addition to water-potential data, stable isotope data from the Nevada Test Site also indicate upward water movement since the last glacial cycle [Tyler *et al.*, 1996]. The effect of upward flow should be examined further with respect to Cl profiles in arid settings.

Various factors may cause violation of the piston flow assumption. The term piston flow, or plug flow, refers to uniform displacement of water in the unsaturated zone by infiltrating water where hydrodynamic dispersion and preferential flow are insignificant. Hydrodynamic dispersion includes the effects of mechanical dispersion as a result of microscopic water-velocity variations and molecular diffusion. Field studies have indicated that in many cases hydrodynamic dispersion minimally affected the results of their studies [Allison and Hughes, 1978; Murphy *et al.*, 1996; Ginn and Murphy, 1997]. However, low water fluxes and long timescales in arid settings can result in diffusion being important, as shown by Peck *et al.* [1981] and Cook *et al.* [1992]. Anion exclusion occurs when Cl is excluded from water associated with the diffuse double layer and only moves in free water. Preferential flow refers to nonuniform water movement in which much of the unsaturated zone is bypassed. Preferential flow is common in fractured rocks, such as fractured tuff at Yucca Mountain [Yang *et al.*, 1996; Fabryka-Martin *et al.*, 1998] and fractured chalk in the Negev Desert [Nativ *et al.*, 1995]. In these fractured systems, preferential flow is generally inferred from deep penetration of bomb-pulse tracers such as ^{36}Cl and ^3H to 440-m depth at Yucca Mountain and bomb-pulse ^3H to 12-m depth at the Negev site. These observations indicate that some of the assumptions associated with the Cl transport process may not be valid. This could result in greatly increased uncertainties in estimated fluxes and ages of pore water. These assumptions should be questioned and tested if necessary at all field sites. Potential problems with the CMB technique underscore the need for independent techniques for estimating water fluxes and dating pore water in arid unsaturated zones.

Several tracers have been used to evaluate flow in thick vadose zones. Chlorine 36 (half-life of 301,000 years) has been used to a limited extent to date pore water in arid unsaturated

zones over timescales ranging from decades to thousands of years and to evaluate preferential flow. Tritium (half life of 12.4 years) has also been used to date pore water up to 40 years old and to evaluate preferential flow. Natural ^3H abundance ranges from about 5 to 10 tritium units (TU) in precipitation in the Northern Hemisphere. Tritium concentrations increased to ≥ 2000 TU during atmospheric nuclear testing [International Atomic Energy Agency, 1983] from 1952 through 1963 in the Northern Hemisphere. Stable isotopes of oxygen and hydrogen are useful in determining the direction of water movement and in estimating upward water fluxes as a result of evaporation.

The primary objective of this study was to evaluate uncertainties in estimating water fluxes and dating pore water in arid unsaturated zones, with particular emphasis on the accuracy of the CMB technique. Radioactive decay of ^{36}Cl was also examined to date pore water. Uncertainties in input, transport processes, and output for meteoric Cl were evaluated using information from Cl and other tracers and hydraulic data. An in-depth analysis of transport processes was conducted by using water-potential and stable isotope data to determine flow direction, and bomb ^3H and bomb ^{36}Cl were used to evaluate preferential flow. In this study, representative Cl profiles from drainage and interdrainage settings in Eagle Flat basin in the Chihuahuan Desert of Texas were used.

2. Site Description

The Eagle Flat basin is a sediment-filled basin within the Basin and Range physiographic province [Scanlon *et al.*, 1999a, b]. The mineralogy of the sediment fill includes quartz, feldspar, amphibole, and calcite derived from Precambrian metamorphic rocks, Permian and Cretaceous sandstones and limestones, and Tertiary volcanic rocks [Jackson *et al.*, 1993]. The unsaturated zone ranges from 198 to 230 m in thickness in the basin. The regional climate is subtropical arid [Larkin and Bomar, 1983]. Mean annual precipitation is 320 mm derived from a 30-year record.

The main geomorphic features are the drainage system, including Blanca Draw and Grayton Lake playa; interdrainage areas, including basin-fill deposits and eolian sheets; and localized topographic depressions, such as a fissure in the interdrainage area [Scanlon *et al.*, 1999a, b]. Blanca Draw, the axial drainage system for Eagle Flat basin, drains into Grayton Lake playa (20 km²), an ephemeral playa that was flooded between May 1992 and October 1993. When not flooded, it is sparsely vegetated. The floor of the playa consists of clay containing mud cracks resulting from shrink/swell of the sediment. An earth fissure, found in the interdrainage area, has a surface expression of about 640 m in length. Water ponds occasionally in this fissure. The fissure, or gully, is underlain by a tension fracture. The fracture extends to a depth of at least 3.5 m; however, the maximum vertical extent is unknown because dug trenches did not reach the base of the fracture.

3. Methods

3.1. Theory

Quantitative interpretation of Cl concentrations is based on applying the continuity equation to Cl transport through the unsaturated zone, which assumes that Cl in the liquid phase does not partition into the solid or gas phases and that Cl is conservative (i.e., no subsurface sources or sinks). A simple form of the CMB approach is generally applied at most sites:

$$q_w = J_{Cl}/c_{Cluz} = Pc_{ClP}/c_{Cluz}, \quad (1)$$

where q_w is the volumetric water flux below the root zone ($L T^{-1}$), J_{Cl} is the Cl mass flux or Cl deposition flux at the surface (input ($M L^{-2} T^{-1}$)), c_{Cluz} is the pore water Cl concentration in the unsaturated zone (output ($M L^{-3}$)), P is precipitation ($L T^{-1}$), and c_{ClP} is the Cl concentration in precipitation (assumed to include dry fallout ($M L^{-3}$)). The Cl mass flux at the surface includes Cl in precipitation and dry fallout. Many precipitation collectors include wet and dry fallout. According to this simplified CMB approach the transport process for Cl is assumed to be 1-D, downward piston transport, and the Cl input is assumed to be constant at the surface.

The age or residence time (t) represented by Cl at depth z can be evaluated by dividing the cumulative total mass of Cl from the surface to that depth by the annual Cl input:

$$t = \frac{1}{J_{Cl}} \int_0^{z_i} \theta(z)c_{Cluz}(z) dz = \frac{1}{J_{Cl}} \int_0^z \rho_b(z)M_{Cluz}(z) dz, \quad (2)$$

where θ is the volumetric water content ($L^3 L^{-3}$), ρ_b is the dry bulk density ($M L^{-3}$), and M is the mass of Cl per mass of dry soil ($M M^{-1}$). The assumptions for estimating age are similar to those for estimating flux with the exception that flow can be upward or downward.

Chlorine 36 has been used to date pore water and to evaluate preferential flow in arid unsaturated zones. Chlorine 36 is produced naturally in the atmosphere [Bentley *et al.*, 1986]. Estimates of water residence time over three different time-scales can be calculated from chlorine 36 data. (1) Bomb-pulse $^{36}Cl/Cl$ ratios have been used to estimate water fluxes up to 40 years old and to evaluate preferential flow [Phillips *et al.*, 1988; Scanlon, 1992; Fabryka-Martin *et al.*, 1993, 1998]. Nuclear weapon tests conducted in the Pacific between 1952 and 1958 resulted in ^{36}Cl concentrations in rainfall that were up to 1000 times greater than natural fallout levels [Bentley *et al.*, 1986]. (2) Variations in $^{36}Cl/Cl$ ratios during the past 40,000 years may also be used as a tracer of water movement [Plummer *et al.*, 1997]. The temporal variations in $^{36}Cl/Cl$ ratios are attributed either to variations in cosmogenic production of ^{36}Cl , which is inversely related to Earth's magnetic field intensity, or to a shift in the jet stream, which determines the latitude at which the peak $^{36}Cl/Cl$ deposition rate occurs. The $^{36}Cl/Cl$ ratios were measured in fossil urine from pack rat middens in Nevada, which were dated by ^{14}C from 38,000 years to present. These data showed increases in $^{36}Cl/Cl$ ratios up to 150 to 200% higher than modern prebomb ratios earlier than 10,000 years ago and ranged from 50 to 100% of modern prebomb ratios during the past 10,000 years. Comparison of the reconstructed ^{36}Cl production with variations in $^{36}Cl/Cl$ in pore water has been used to estimate ages of water at the Nevada Test Site [Tyler *et al.*, 1996]. (3) Radioactive decay of ^{36}Cl can also be used to estimate water ages up to 1,000,000 years. The residence time of the pore water (t) is calculated as follows:

$$t = -\frac{1}{\lambda_{36}} \ln \frac{R - R_{se}}{R_0 - R_{se}} \quad (3)$$

where λ_{36} is the decay constant for ^{36}Cl ($2.30 \times 10^{-6} \text{ yr}^{-1}$), R is the measured $^{36}Cl/Cl$ ratio, R_{se} is the secular equilibrium $^{36}Cl/Cl$ ratio ($\sim 10 \times 10^{-15}$) [Bentley *et al.*, 1986], and R_0 is the initial $^{36}Cl/Cl$ ratio.

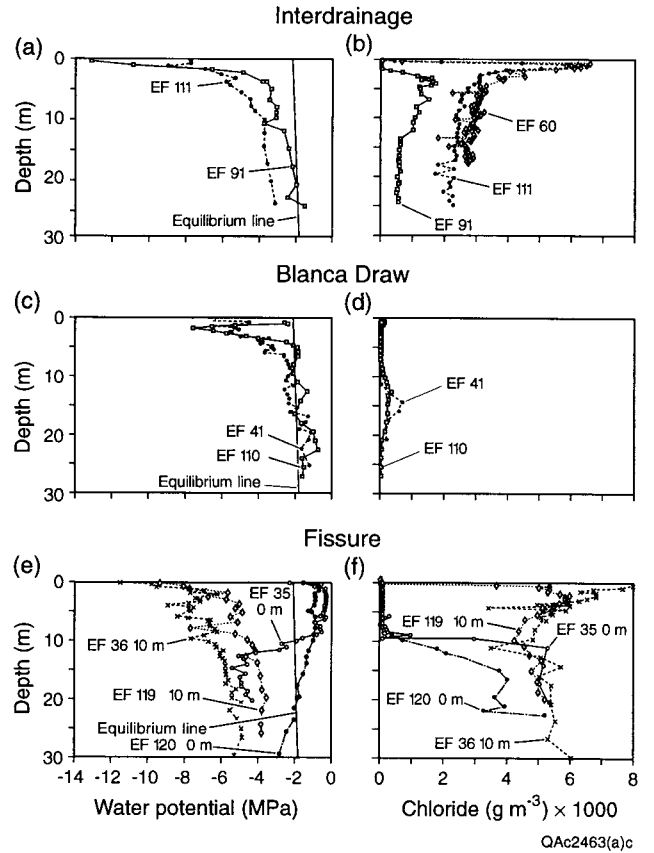


Figure 1. (a, c, and e) Water potential and (b, d, and f) Cl concentrations in pore water in interdrainage profiles (EF 60, EF 91, and EF 111), drainage profiles (Blanca Draw EF 41 and EF 110), and fissure (EF 35, EF 36, EF 119, and EF 120). The equilibrium line represents the no-flow line in which water potential and gravitational potential are balanced (i.e., water potential equals negative gravitational potential).

3.2. Field and Laboratory Procedures

Representative profiles of environmental tracers from a maximum of 50 different profiles from the Eagle Flat basin described by Scanlon *et al.* [1999a, b] were used to evaluate uncertainties in estimating water flux and dating pore water. Sediment samples from these boreholes were analyzed for water content, water potential, and Cl (Figure 1). Gravimetric water content was determined by weighing and oven drying the samples at $105^{\circ}C$ for 24 hours. This procedure may have resulted in removal of some bound water from clays. Water potential was measured in the laboratory using a thermocouple psychrometer with sample changer (model SC-10A, Decagon Devices, Inc., Pullman, Washington). To determine Cl content, double-deionized water was added to the dried sediment sample in a 3:1 ratio by weight. Samples were agitated on a reciprocal shaker table for 4 hours. The supernatant was filtered through $0.45\text{-}\mu m$ filters. Cl was then analyzed by ion chromatography (IC) for concentrations generally $\leq 20 \text{ g m}^{-3}$ or by potentiometric titration for concentrations generally $> 20 \text{ g m}^{-3}$. Cl concentrations are expressed as grams of Cl per cubic meter of pore water (equivalent to milligrams of Cl per liter of pore water). Cl/Br ratios were measured in 14 samples from the surface to 21 m depth from borehole EF 61. Both ions were analyzed using IC by HydroGeoChem Inc. (Tucson, Arizona).

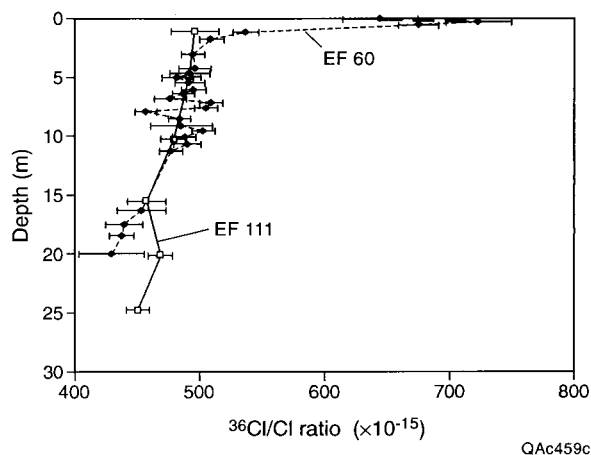


Figure 2. Vertical $^{36}\text{Cl}/\text{Cl}$ profiles in interdrainage areas (EF 60 and EF 111). Error bars represent 1σ analytical uncertainties in $^{36}\text{Cl}/\text{Cl}$ measurements calculated according to *Elmore et al.* [1984].

Cl and Br concentrations were measured by IC by Los Alamos National Laboratory in 16 precipitation samples collected at the site approximately monthly during 1996 and 1997. Some months had no rain.

The $^{36}\text{Cl}/\text{Cl}$ ratios were measured in samples from boreholes EF 60, EF 111 (interdrainage area), EF 92, EF 96 (beneath and 10 m from fissure), and GL 2 (Grayton Lake playa) by accelerator mass spectrometry at Lawrence Livermore National Laboratory according to procedures outlined by *Elmore et al.* [1979]. Preparation of ^{36}Cl samples for analysis followed procedures outlined by *Mattick et al.* [1987].

Samples for ^3H analysis were collected from boreholes EF 79, EF 117 (interdrainage area), EF 92, EF 96 (beneath and 10 m from fissure), and GL 2 (Grayton Lake playa). The water was extracted from the core samples in the laboratory by toluene azeotropic distillation. The pore water samples were electrolytically enriched and analyzed by liquid scintillation at the University of Arizona Tritium Laboratory or by gas proportional counting at the University of Miami Tritium Laboratory.

Water was analyzed for $\delta^2\text{H}$ and $\delta^{18}\text{O}$ by the Desert Research Institute (University of Nevada, Las Vegas) on samples from EF 64, EF 91, EF 113 (interdrainage area), GL 2 (Grayton Lake), GL 4 (adjacent to Grayton Lake), EF 92, and EF 96 (beneath and 10 m from fissure) and on 16 precipitation samples collected during 1996 and 1997. Water was extracted for analysis from approximately 100 g of sediment by toluene extraction [*Ingraham and Shadel*, 1992]. Results of isotopic analysis are reported in standard delta notation, with respect to Vienna standard mean ocean water (VSMOW).

4. Results and Discussion

Representative Cl profiles in interdrainage and drainage areas and beneath the fissure from the Eagle Flat basin were used to evaluate water fluxes and ages. Borehole locations and detailed results of all sampling are given by *Scanlon et al.* [1999a, b]. Residence times based on $^{36}\text{Cl}/\text{Cl}$ ratios are discussed first, then uncertainties related to the CMB technique are evaluated, including uncertainties in Cl input and Cl output and in transport mechanisms. The effect of these uncertainties on water fluxes and ages calculated by the CMB technique is then described.

4.1. Residence Time Based on ^{36}Cl Data

Detailed sampling for ^{36}Cl analysis was conducted in EF 60 to test for variations in $^{36}\text{Cl}/\text{Cl}$ ratios (Figure 2). The CMB age for this profile is 91,000 years at 17.5 m depth (equation (2)) on the basis of a Cl input of $87\text{ mg m}^{-2}\text{ yr}^{-1}$ that is discussed in section 4.2. This CMB age spans the time period in which secular variations in $^{36}\text{Cl}/\text{Cl}$ were suggested by *Plummer et al.* [1997]. These variations were attributed either to variations in cosmogenic production of ^{36}Cl or to a shift in the jet stream. Measured $^{36}\text{Cl}/\text{Cl}$ ratios in the EF 60 profile were decay corrected according to the CMB age and compared with measured $^{36}\text{Cl}/\text{Cl}$ ratios in urine from pack rat middens in Nevada and with the reconstructed $^{36}\text{Cl}/\text{Cl}$ [*Guyodo and Valet*, 1996] and ^{14}C production [*Plummer et al.*, 1997] (Figure 3). There is no systematic variation in $^{36}\text{Cl}/\text{Cl}$ ratios over this time in the EF 60 profile. Either the deposition flux of $^{36}\text{Cl}/\text{Cl}$ did not vary over this time at this location, or the variations were not preserved in this profile, possibly because of diffusion. The effect of diffusion is discussed in more detail in section 4.3.4. Although sampling for ^{36}Cl in the EF 111 profile is less detailed than that in EF 60, decay-corrected $^{36}\text{Cl}/\text{Cl}$ ratios from EF 111 also do not vary over time. Therefore variations in cosmogenic production of ^{36}Cl could not be used to date pore water in this basin.

Use of radioactive decay of ^{36}Cl to date pore water was also evaluated. High $^{36}\text{Cl}/\text{Cl}$ ratios ($537\text{--}723 \times 10^{-15}$) in the upper 1.2 m of the EF 60 profile probably reflect the tail of the bomb-pulse signal (Figure 2). Ratios of $^{36}\text{Cl}/\text{Cl}$ do not vary systematically from 1.8- to 10.7-m depth and have a mean value of $491 \times 10^{-15} \pm 12 \times 10^{-15}$ in this zone. Ratios of $^{36}\text{Cl}/\text{Cl}$ decrease gradually from 491×10^{-15} at 10.7-m depth to 430×10^{-15} at 20-m depth. Assuming the decrease is due solely to radioactive decay, then the residence time of the pore water corresponding to this decay is 59,000 years. This decay age compares favorably with the CMB age of 55,000 years for the same depth interval. Propagation of errors resulting from 1σ uncertainties in the $^{36}\text{Cl}/\text{Cl}$ analyses results in a 1σ uncertainty in age of 28,700 years (Appendix A). The analytical uncertainty associated with the $^{36}\text{Cl}/\text{Cl}$ ratio at 20-m depth is unusually high at 6%, whereas that for 70% of the samples and the next shallower sample is 2%. This reduction in analytical uncertainty would reduce the uncertainty in age to 14,400 years. The $^{36}\text{Cl}/\text{Cl}$ ratios decreased from 491×10^{-15} at 5-m depth in EF 111 in the interdrainage area to 450×10^{-15} at 25-m depth, which suggests a residence time of $39,000 \pm 13,000$ years, based on radioactive decay. The residence time is much less than that estimated by CMB analysis (105,000 years) for the EF 111 profile. The discrepancy between decay age and CMB age for the EF 111 profile probably reflects uncertainties in both techniques.

It may be argued that the decay of ^{36}Cl with depth and the calculated ages are not significant because of the large errors in the $^{36}\text{Cl}/\text{Cl}$ ratios; however, the slopes of the lines relating $^{36}\text{Cl}/\text{Cl}$ ratios and age to depth were significantly different from 0 in both profiles ($\alpha = 0.05$) [*Taylor*, 1982]. Increases in the deposition flux of ^{36}Cl by up to a factor of 2, as suggested by data from Nevada [*Plummer et al.*, 1997], or subsequent diffusion of the ^{36}Cl would result in increased decay ages. The residence times based on radioactive decay of ^{36}Cl ($39,000 \pm 13,000$ to $59,000 \pm 14,400$ years) represent the lower limit of applicability of this technique because of analytical uncertainties in the measurement of $^{36}\text{Cl}/\text{Cl}$ ratios (Figure 4). Percent

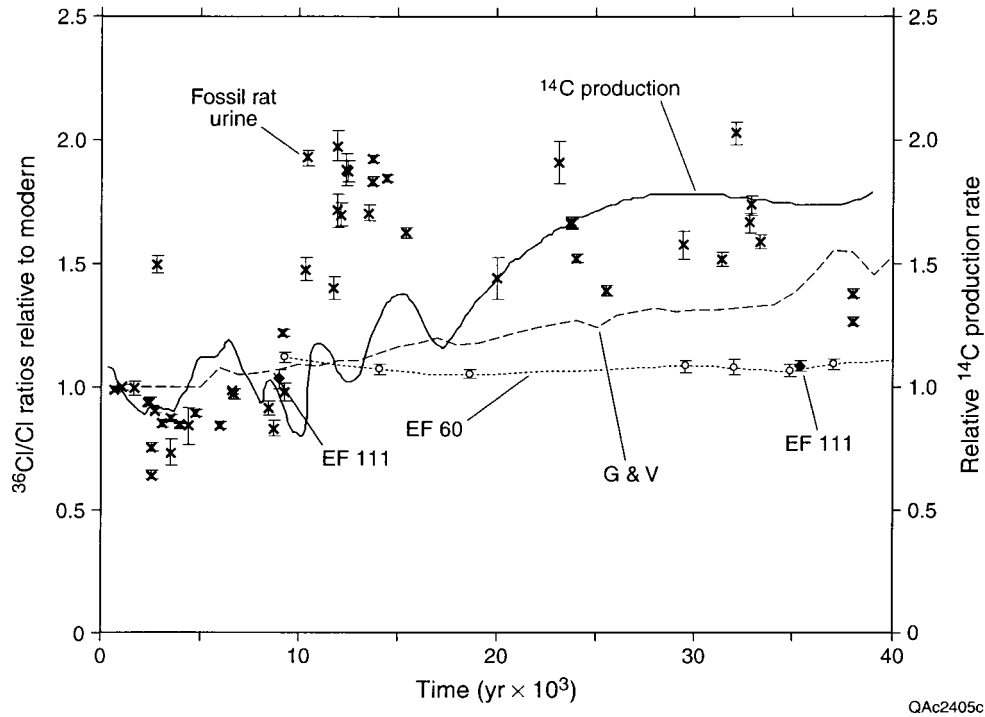


Figure 3. Decay-corrected $^{36}\text{Cl}/\text{Cl}$ ratios using the chloride mass balance age relative to the modern $^{36}\text{Cl}/\text{Cl}$ ratio at the site (491×10^{-15}) in interdrainage areas (EF 60 and EF 111); $^{36}\text{Cl}/\text{Cl}$ ratios in urine from pack rat middens; reconstructed $^{36}\text{Cl}/\text{Cl}$ ratios [Guyodo and Valet, 1996]; and reconstructed ^{14}C production (based on Plummer *et al.* [1997]) from cosmic production as influenced by variations in the geomagnetic field intensity.

uncertainty in residence time increases sharply as residence time decreases. The $^{36}\text{Cl}/\text{Cl}$ radioactive decay data are used only as corroborative evidence for the CMB ages in this study. Both techniques indicate long pore water residence times in interdrainage settings.

4.2. Uncertainties in Cl Input and Output

Cl input or Cl mass deposition flux can be estimated from (1) ^{36}Cl data or (2) direct measurements of Cl concentrations in precipitation and dry fallout multiplied by the mean annual precipitation (320 mm yr^{-1}). The Cl input ($87 \text{ mg m}^{-2} \text{ yr}^{-1}$) was calculated by dividing the atmospheric fallout of ^{36}Cl ($^{36}\text{Cl}_a$) for the latitude of the site ($23 \text{ atoms m}^{-2} \text{ s}^{-1}$ [Bentley

et al., 1986]) by the measured prebomb $^{36}\text{Cl}/\text{Cl}$ ratio (samples from 1.8 to 10.7 m in borehole EF 60 (491×10^{-15} , $^{36}\text{Cl}/\text{Cl}_0$)) according to the following equation:

$$J_{\text{Cl}} = \frac{^{36}\text{Cl}_a (\text{atoms m}^{-2} \text{ s}^{-1}) (31.558 \times 10^6 \text{ s yr}^{-1}) (35.5 \times 10^3 \text{ mg mol}^{-1})}{^{36}\text{Cl}/\text{Cl}_0 (6.023 \times 10^{23} \text{ atoms mol}^{-1})} \tag{4}$$

This Cl input ($87 \text{ mg m}^{-2} \text{ yr}^{-1}$) is similar to values estimated by Phillips [1994] for sites in New Mexico (75 to $125 \text{ mg m}^{-2} \text{ yr}^{-1}$) and is equivalent to a Cl concentration in precipitation and dry fallout of 0.27 g m^{-3} that is based on a long-term mean annual precipitation of 320 mm . In this study, Cl concentrations in precipitation and dry fallout were measured approximately monthly for only 2 years and resulted in a precipitation-weighted average Cl concentration of $0.14 \pm 0.03 \text{ g m}^{-3}$ (equal to Cl deposition flux of $45 \text{ mg m}^{-2} \text{ yr}^{-1}$), which is about half that estimated from the ^{36}Cl data (0.27 g m^{-3}). The Cl input estimated from the ^{36}Cl data is considered more valid for this study than direct measurements of Cl in precipitation and dry fallout because it represents a long time period.

Because sediments in the Eagle Flat basin are alluvial and eolian in origin, it is unlikely that there are any sources of Cl in the subsurface. Cl concentrations in pore water are much lower than those at which halite would precipitate from a saline brine ($\sim 220,000 \text{ g m}^{-3}$ [Holser, 1979]); therefore it is unlikely that there is any Cl in the solid phase. Cl/Br ratios measured in samples from EF 61 in an interdrainage area (92 to 150) are similar to measured Cl/Br ratios in precipitation (24 to 167) and are typical of meteoric Cl [Davis *et al.*, 1998]. In contrast,

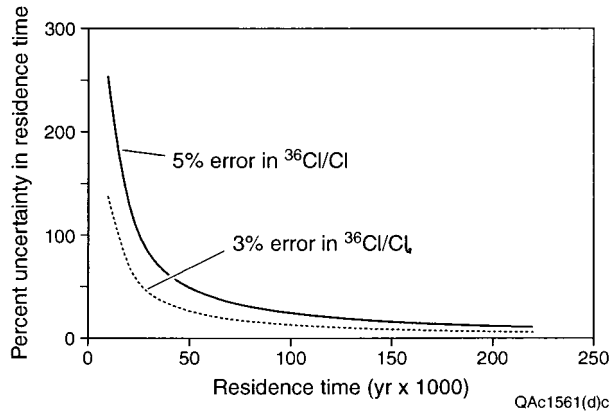


Figure 4. Uncertainties in pore water residence time as a result of analytical uncertainties (1σ) in $^{36}\text{Cl}/\text{Cl}$ measurements (Appendix A).

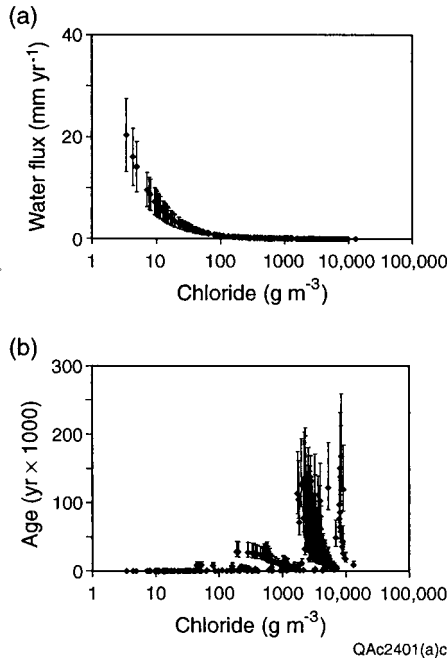


Figure 5. Uncertainties in (a) water flux and (b) age resulting from $\pm 35\%$ uncertainty in Cl input in samples from profiles in drainage and fissure areas (EF 94, EF 110, EF 120, and GL 2) and interdrainage (EF 28, EF 60, EF 66, EF 91, and EF 111) areas.

Cl/Br ratios in samples affected by halite dissolution typically range from 1000 to 10,000 [Davis *et al.*, 1998]. The low Cl/Br ratios in the study area also preclude the Salt Flat playa (~ 25 km northeast of the site) as a source of airborne Cl at the site. Studies by Reheis and Kihl [1995] and Wood and Sanford [1995b] suggest that most of the salt removed by deflation of playas is deposited close to the source. The $^{36}\text{Cl}/\text{Cl}$ ratio measured in a salt sample was 88×10^{-15} , which is lower than the ratios in any of the profiles in the study area (383 to 723×10^{-15}) and suggests negligible contribution of Cl from the Salt Flat. The Cl sample from the Salt Flat was derived partly from Permian salt, which has no ^{36}Cl . The low ratio is attributed to mixing of this Permian Cl with meteoric ^{36}Cl in the groundwater and in situ production near the surface because of capture of cosmogenic neutrons [Fabryka-Martin, 1988]. The low ratio is similar to $^{36}\text{Cl}/\text{Cl}$ ratios measured in salt basins ($< 100 \times 10^{-15}$ [Phillips *et al.*, 1995]).

Uncertainties in the Cl input were estimated from uncertainties in the atmospheric fallout of ^{36}Cl and in the measured prebomb $^{36}\text{Cl}/\text{Cl}$ ratios. Theoretical estimates of natural ^{36}Cl fallout calculated by Lal and Peters [1967] are lower by a factor of 0.7 than those estimated by Bentley *et al.* [1986]. Estimates of ^{36}Cl fallout are being revised by Phillips [1999] to include variations in ^{36}Cl fallout with precipitation [Hainsworth *et al.*, 1994; Knies, 1995]. Although revised ^{36}Cl fallout estimates differ markedly from original estimates by Bentley *et al.* [1986] in many areas, the two estimates are almost identical at our site [Phillips, 1999]. The uncertainty in ^{36}Cl fallout is therefore estimated to be about 30%, which is based on the 30% difference between fallout estimated by Lal and Peters [1967] and fallout estimated by Bentley *et al.* [1986] and Phillips [1999]. Uncertainties in prebomb $^{36}\text{Cl}/\text{Cl}$ ratios are much less than uncertainties in atmospheric fallout of ^{36}Cl . The prebomb

$^{36}\text{Cl}/\text{Cl}$ ratios in widely separated profiles in Eagle Flat basin (EF 60 and EF 111, ~ 2 km apart) are essentially the same (491×10^{-15}). Uncertainty in the prebomb ratio ($\sim 5\%$) includes analytical uncertainty in $^{36}\text{Cl}/\text{Cl}$ measurements ($\sim 3\%$) and uncertainty around the mean value calculated for the EF 60 profile from 1.8- to 10.7-m depth ($1 \sigma = 2\%$). The combined effect of errors in ^{36}Cl fallout (30%) and in prebomb $^{36}\text{Cl}/\text{Cl}$ ratios (5%) results in 35% uncertainty in Cl input. The relationship between water flux and Cl input is linear (equation (1)); therefore $\pm 35\%$ uncertainty in Cl input results in $\pm 35\%$ uncertainty in the water flux. The inverse relationship between age and Cl input results in asymmetric error bars in age from uncertainty in Cl input that range from -26 to 54% (Figure 5 and Table 1) (see Appendix B).

Uncertainties in Cl input are much greater in drainage areas because the amount of run-on and Cl concentrations in run-on are unknown. Cl concentrations in run-on are expected to be greater than those in precipitation because of leaching of Cl from surface soils. The simple CMB equation was modified by Wood and Sanford [1995a] to include the effects of run-on into playas

$$q_w = \frac{Pc_{\text{ClP}}}{c_{\text{Cluz}}} + R_{\text{on}} \left(\frac{A_b c_{\text{ClR}_{\text{on}}}}{A_f c_{\text{Cluz}}} \right), \quad (5)$$

where $c_{\text{ClR}_{\text{on}}}$ is Cl concentration in run-on, R_{on} is run-on, A_b is area of the basin, and A_f is area of the playa floor. Applying (5) to Grayton Lake playa ($R_{\text{on}} \sim 10\%$ of precipitation, A_b , 500 km²; A_f is 20 km²; $c_{\text{ClR}_{\text{on}}}$ is ~ 5 times that in precipitation (1.4 g m^{-3})) results in an order of magnitude increase in the water flux. Similar order-of-magnitude increases in water flux were estimated for playas in north central Texas by including run-on [Scanlon and Goldsmith, 1997]. Many of the parameters in (5) are highly uncertain, such as the amount of run-on, the area contributing run-on, and the Cl concentration in run-on. Water fluxes estimated from the simple CMB approach (equation (1)), which ignores run-on, may underestimate actual water fluxes in arid regions by an order of magnitude (Table 1). Ignoring run-on will result in overestimation of age by about an order of magnitude also, as shown in the following equation:

$$t = \int_0^z \theta c_{\text{Cluz}} dz / P c_{\text{ClP}} + R_{\text{on}} \left(\frac{A_b c_{\text{ClR}_{\text{on}}}}{A_f c_{\text{Cluz}}} \right) c_{\text{Cluz}}, \quad (6)$$

Uncertainties in Cl output result from analytical uncertainties in Cl measurements. Cl concentrations in the supernatant of less than 20 mg L^{-1} were generally measured by ion chromatography ($\pm 0.1 \text{ mg L}^{-1}$), whereas those greater than 20 mg L^{-1} were generally measured by potentiometric titration ($\pm 2 \text{ mg L}^{-1}$). Uncertainties in water flux and age resulting from these uncertainties in output or Cl concentration measurements are shown in Figure 6 and derived in Appendix B. The inverse relationship between flux and Cl output (equation (1)) results in asymmetric error bars in flux when uncertainties in Cl output are large. In interdrainage areas the mean uncertainty in Cl output (3%) results in $\pm 3\%$ uncertainty in flux. The uncertainty range of 0.5 to 10% in Cl output results in $\pm 0.5\%$ uncertainty in flux from the lower bound (0.5%) to -11 to 9% uncertainty in flux from the upper bound (10%). In interdrainage areas the uncertainty in age from uncertainties in Cl output is small (mean $\pm 2\%$ and range 1 to 5%). In drainage areas, uncertainties in Cl output (mean $\pm 12\%$ and range 0.5 to 83%) result in -11 to 13% uncertainty in average water flux (range

Table 1. Uncertainties in Water Flux and Age Based on the Chloride Mass Balance (CMB) Method Resulting From Uncertainties in Cl input, Cl output, and Transport Processes for Profiles in Interdrainage (EF 28, EF 60, EF 66, EF 91, and EF 111) and Drainage and Fissure Areas (EF 94, EF 110, EF 120, and GL 2)

	Interdrainage Areas		Drainage Areas	
	Water Flux	Age	Water Flux	Age
Cl input	±35%	-26 to 54%	~10×	~0.1×
Cl output	±3% (±0.5, -9 to +11%)	±2% (±1 to ±5%)	-11 to +13% (±0.5%; -45 to 479%)	±7% (±1 to ±20%)
Combined (Cl input plus output)	±38% (±35.5%; -44 to +46%)	-24 to 56% (-25 to 59%)		
Transport				
One Dimensional	yes	yes	yes/no*	yes/no*
Downward	yes/no†	yes/no†	yes	yes
Preferential flow	no	no	yes	yes
Diffusion	yes	yes	no	no
Overall CMB	upper bound ±38%	lower bound -21 to 45%	lower bound -11 to 13%‡	upper bound ±7%‡

The uncertainty in the Cl input was estimated to be 35% in interdrainage areas and an order of magnitude in the drainage areas (including the fissure). Analytical uncertainties in Cl output concentration measurements ranged from 0.5 to 10% (mean 3%) in interdrainage areas and from 0.5 to 83% (mean 12%) in drainage areas. Because Table 1 may be confusing, the following example is provided for clarity. For example, the mean error in Cl output (3%) results in ±3% uncertainty in water flux. The range in error in Cl output (0.5 to 10%) results in a range in error in water flux from ±0.5% to -9 to +11%. The asymmetry in the error bar is attributed to the inverse relationship between water flux and Cl. The asymmetry increases as the error increases.

*Flow is generally 1-D beneath drainage areas; however, there is some evidence of 2-D flow (lateral flow) adjacent to drainage areas.

†Flow may be upward in the shallow zone and is assumed to be downward at greater depth (≥10 m).

‡CMB approach underestimates water flux and overestimates age by about an order of magnitude because of neglecting Cl in run-on.

±0.5 to -45 to 479%) and ±7% uncertainty in age (range ±1 to ±20%) (Table 1). Uncertainties in Cl output result in the CMB water fluxes being less accurate at high water fluxes because Cl concentrations are less sensitive to water fluxes at these low concentrations. Sensitivity lessens partly as a result of the inverse relationship between water flux and Cl (equation (1)), and the effect of analytical uncertainty in water flux increases as the Cl concentrations decrease. Small changes in Cl

concentration result in large changes in water flux at low Cl concentrations.

4.3. Uncertainties in Cl Transport Mechanisms

The CMB approach requires that Cl must be transported by 1-D, downward piston flow. Uncertainties in transport mechanisms were therefore evaluated.

4.3.1. Flow direction. Although the CMB approach assumes that water moves downward, water-potential data indicate that downward water movement is restricted to areas that pond water and that all other areas have upward water movement. Uniformly high water potentials beneath the fissure that plot to the right of the equilibrium line (equilibrium between water potential and gravitational potential) indicate downward water movement in the upper 10 to 20 m (Figure 1e). In contrast, water-potential data in interdrainage and shallow drainage areas indicate upward water movement (Figures 1a and 1c). Water potentials are higher (less negative) at depth and decrease toward the surface (more negative). This upward decrease in water potentials indicates an upward driving force for water movement at these locations. Water potentials plot to the left of the equilibrium line, also indicating a potential for upward water flow under steady state conditions. In the Blanca Draw drainage area, upward water-potential gradients are restricted to the upper 6 to 15 m; at greater depths, water potentials plotted to the right of the equilibrium line, indicating drainage (Figure 1c).

The timescales represented by the upward water potentials are difficult to assess. In the drainage area, upward water-potential gradients in the upper 6 to 15 m coexist with low Cl concentrations, suggesting that the upward water potentials were developed over fairly short time periods that were insufficient to accumulate significant amounts of Cl (Figures 1c and 1d). The water-potential data represent current drying conditions, whereas the Cl data represent higher water fluxes in the past that flushed out Cl. The drainage area has dense mesquite trees that have deep roots and can readily evapotranspire wa-

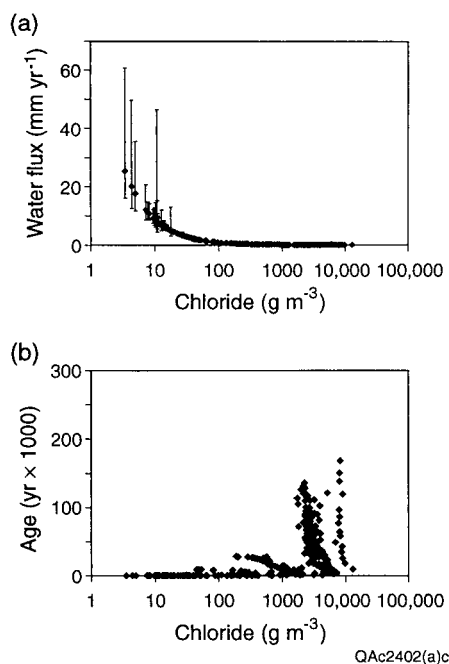


Figure 6. Uncertainties in (a) water flux and (b) age resulting from analytical uncertainties in Cl measurements in samples from profiles in drainage and fissure areas (EF 94, EF 110, EF 120, and GL 2) and interdrainage areas (EF 28, EF 60, EF 66, EF 91, and EF 111).

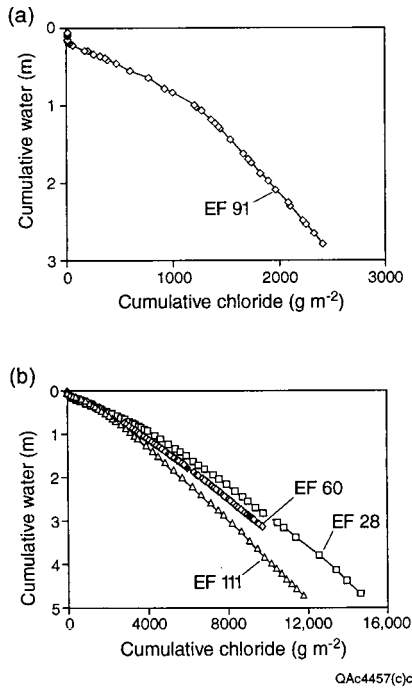


Figure 7. Cumulative water versus cumulative Cl for (a) EF 91 and (b) EF 28, EF 60, and EF 111 profiles in interdrainage areas.

ter from depth. Data from the drainage area therefore indicate that upward water-potential gradients are not necessarily inconsistent with long-term net downward water movement. In interdrainage areas the upward water-potential gradients may represent drying over much longer time periods and are consistent with Cl accumulation near the surface (Figure 1b). Plots of cumulative Cl versus cumulative water content (Figure 7) can be used to evaluate changing conditions over time. The plot for EF 91 shows an increase in slope (Figure 7a) that corresponds to a CMB age of about 11,000 years, similar to some other profiles in the eolian sheet [Scanlon *et al.*, 1999a, b]. Higher water fluxes prior to that time correspond to Pleistocene time. The reduced slope in the Holocene may reflect reduced water flux or change in flux direction from downward (Pleistocene) to upward (Holocene). The other profiles in the

interdrainage area do not show any response to Pleistocene climate change (Figure 7b) and represent very long time periods. It is unlikely that upward water fluxes have persisted for the entire time period represented by these Cl profiles (such as 136,000 years for EF 111 profile). If they did, we would not expect to see radioactive decay of $^{36}\text{Cl}/\text{Cl}$, which is found in those profiles. The time period represented by the upward water potential profiles is therefore estimated to be less than $\sim 10,000$ years, or Holocene age.

The subsurface distributions of $\delta^2\text{H}$ and $\delta^{18}\text{O}$ were also used to evaluate the direction of water movement. Data from beneath and adjacent to Grayton Lake playa plot parallel to the local meteoric water line (slope 6.3), indicating no recent evaporation (Figure 8a). The profile beneath the fissure (EF 92) also shows no enrichment in $\delta^{18}\text{O}$ relative to $\delta^2\text{H}$ except at the shallowest depth. The stable isotope data adjacent to the fissure are similar to those in other interdrainage areas. Interdrainage profiles show enrichment of $\delta^{18}\text{O}$ relative to $\delta^2\text{H}$ that is described by $\delta^2\text{H} = 3.1 \delta^{18}\text{O} - 38$ (Figure 8b). This low slope is consistent with evaporation of pore water in the unsaturated zone, similar to slopes determined by Allison [1982] for evaporation from dry soils. This evaporation line intersects the local meteoric water line at a position more depleted than that of the mean modern precipitation or mean winter precipitation, suggesting downward water flux during a cooler, wetter climate (Pleistocene times). This situation is consistent with that of the Cl data just discussed. Vertical profiles of $\delta^2\text{H}$ and $\delta^{18}\text{O}$ generally show the most isotopic enrichment near the surface (Figures 9a and 9b).

The stable isotope data were used to calculate subsurface evaporation rates in interdrainage areas (1) from the position of the isotopic peak and (2) from “the decay length method in the liquid transport region” [Barnes and Allison, 1983, 1988]. The depths of the isotopic peaks were similar for $\delta^2\text{H}$ and $\delta^{18}\text{O}$ in EF 64 (3.2 m) and in EF 91 (3.0 m). Evaporation rates calculated according to the position of the isotopic peak ranged from 0.3 to 0.4 mm yr^{-1} (Appendix C). The “decay length method” assumes equilibrium between upward advection of isotopically depleted water and downward diffusion of enriched water for each isotope, resulting in exponential profiles. Evaporation rates based on this method ranged from 0.2 mm yr^{-1} (EF 64) to 0.3 to 0.5 mm yr^{-1} (EF 91). The calculated

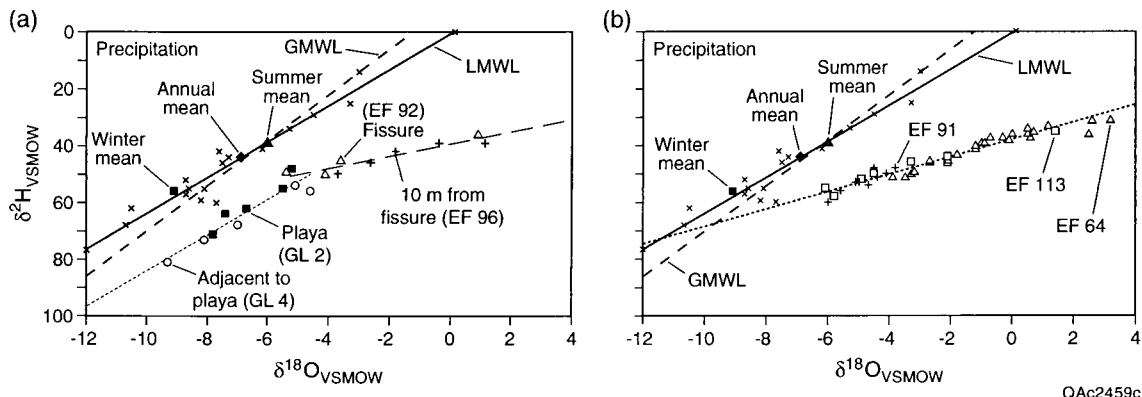


Figure 8. The $\delta^2\text{H}$ versus $\delta^{18}\text{O}$ plot including data from (a) beneath and adjacent to the fissure (EF 92 and EF 96) and beneath and adjacent to Grayton Lake playa (GL 2 and GL 4) and (b) interdrainage profiles (EF 64, EF 91, and EF 113). The local meteoric water line (LMWL) was calculated from precipitation data collected \sim monthly for 2 years. The standard error for $\delta^2\text{H}$ analyses is $\pm 1\text{‰}$ and for $\delta^{18}\text{O}$ analyses is $\pm 0.2\text{‰}$.

upward water fluxes are high and may primarily reflect evaporation of water in the near-surface root zone.

These stable isotope data indicate that the sediments are drying and are consistent with the upward water-potential gradients. Upward movement of water in the liquid phase would reduce CMB ages because of the additional source of Cl in the denominator of equation (2). The upward water flux can also be used to explain the high Cl concentrations in the shallow subsurface and the decrease in Cl concentrations at greater depths. Cl is accumulating in the near surface because of drying of the profile and addition of Cl at the surface, which is substantiated by the cumulative Cl versus water plots and the stable isotope data. Therefore the CMB approach should not be used in the shallow zone where Cl is accumulating and where concentration gradients are steep but rather should be restricted to the deeper zones of the profiles ($\sim \geq 10$ m).

4.3.2. One-dimensional flow. Because the topography of the Eagle Flat basin is fairly flat, subsurface lateral flow as a result of surface topographic variations is expected to be minimal. However, water may move laterally through layered or heterogeneous sediments. Cl profiles in interdrainage areas do not provide any indication of lateral flow, nor do calcic soil horizons seem to affect water movement. Geologic data indicate that they are fractured and consist of stage III carbonate [Jackson *et al.*, 1993; Langford, 1993].

The only evidence of lateral flow was found in areas of ponded water, such as the fissure. The steepness of the Cl and water-potential fronts at a depth of about 10 m beneath the fissure (EF 35) is attributed to the natural capillary barrier effect of layered sediments (Figures 1e and 1f) [Scanlon *et al.*, 1997a]. Dilution of Cl in the profile 10 m from the fissure (EF 36) by about 30% at approximately the depth of the Cl front in the profile beneath the fissure is attributed to lateral flow. Lateral flow was also shown in a dye-tracing experiment in

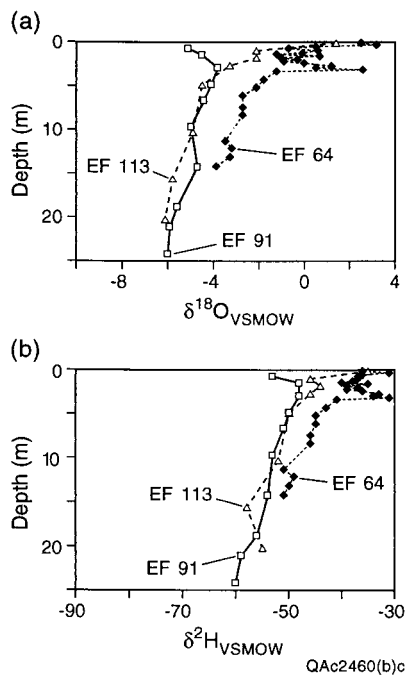


Figure 9. Depth profiles in (a) $\delta^{18}\text{O}$ and (b) $\delta^2\text{H}$ in pore water samples from boreholes EF 64, EF 91, and EF 113 in interdrainage areas.

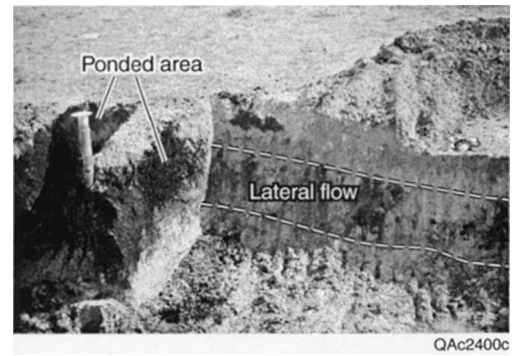


Figure 10. Lateral flow beneath the Eagle Flat fissure, shown by dye-tracing experiment.

which a 2-m² area was ponded for 8 hours by water containing FD&C blue dye [Scanlon *et al.*, 1999a]. Excavation beneath and adjacent to the ponded area revealed dye at distances of ~ 5 m from the ponded area (Figure 10). These data suggest that the no-lateral-flow assumption may not be valid in areas where water ponds. Subsurface lateral flow should not affect the calculated CMB water flux beneath the ponded area because Cl concentrations in pore water are not affected, but it would affect the calculated water flux adjacent to the ponded areas; therefore one should use caution when calculating water fluxes in areas adjacent to ponded regions.

4.3.3. Preferential flow. Pulse-type tracers such as bomb ^3H and bomb ^{36}Cl are generally used to evaluate whether water is moving preferentially. In an interdrainage profile (EF 79), high ^3H concentrations in the upper 5 m probably reflect the tail of the bomb pulse (Figure 11a), and ^3H levels below this zone were low (EF 79 and EF 117 with range 0.14 ± 0.24 to 1.71 ± 0.44 TU ($\pm 2\sigma$)). In some cases the ^3H levels were less than the 2σ error, indicating no ^3H . The ^3H level in a procedural blank (0.98 ± 0.5 TU, ^3H -free water added to an oven-dried sample) was similar to ^3H levels found in EF 79 and EF 117 profiles at depth and indicates no ^3H in these settings. The lack of ^3H is consistent with measured high Cl concentrations and estimated low water fluxes for these sediments and indicates that there is no preferential flow in these interdrainage profiles or else that ^3H is not a good tracer for such flow in these settings. In contrast, high ^3H levels beneath and adjacent to the fissure (7 to 33 TU) and beneath Grayton Lake playa (5 to 12 TU) indicate preferential flow (Figure 11a). Preferential flow is expected beneath Grayton Lake playa because large desiccation cracks develop during dry periods.

In contrast to the ^3H data, measured $^{36}\text{Cl}/\text{Cl}$ ratios beneath the fissure and beneath Grayton Lake playa are low (290 to 530×10^{-15}) and do not provide evidence of preferential flow (Figure 11b). Typical bomb-pulse $^{36}\text{Cl}/\text{Cl}$ ratios are about an order of magnitude higher [Phillips *et al.*, 1988; Scanlon, 1992]. Because $^{36}\text{Cl}/\text{Cl}$ ratios are measured in core samples that contain a component of preferentially moving water and water in the matrix, mixing of water moving preferentially and in the matrix may account for the low $^{36}\text{Cl}/\text{Cl}$ ratios. The measured $^{36}\text{Cl}/\text{Cl}$ ratio in a mixed sample (subscript mix) can be calculated as follows:

$$^{36}\text{Cl}/\text{Cl}_{\text{mix}} = \frac{V_p \text{Cl}_p ^{36}\text{Cl}/\text{Cl}_p + V_m \text{Cl}_m ^{36}\text{Cl}/\text{Cl}_m}{V_p \text{Cl}_p + V_m \text{Cl}_m} \quad (7)$$

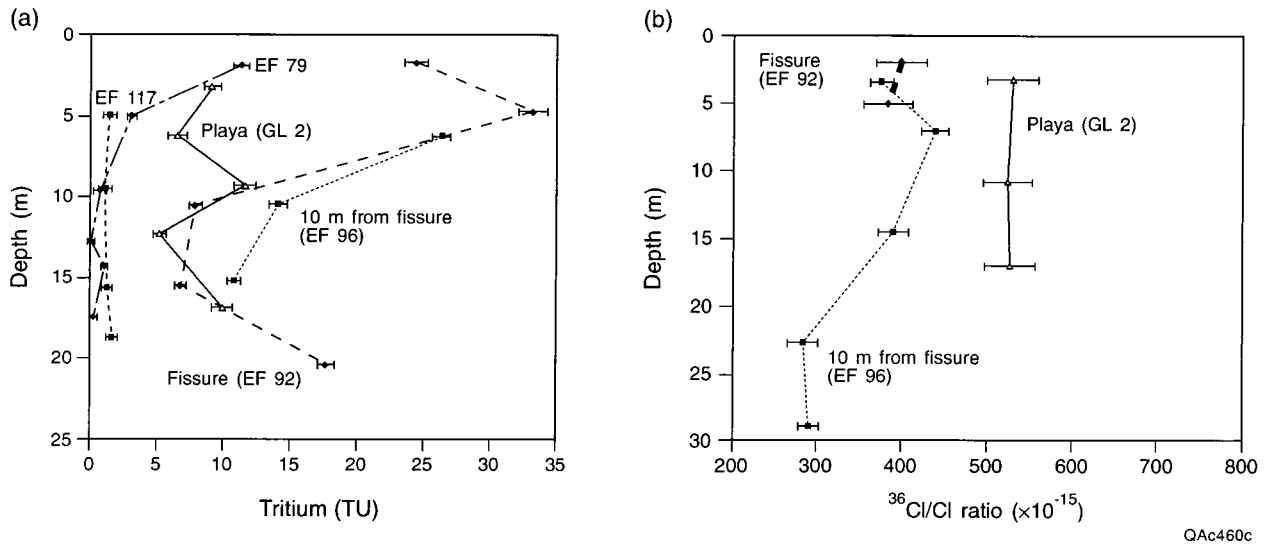


Figure 11. Vertical profiles in (a) tritium concentrations in interdrainage areas (EF 79 and EF 117), beneath (EF 92) and 10 m from the fissure (EF 96) and beneath Grayton Lake (GL 2) and (b) $^{36}\text{Cl}/\text{Cl}$ ratios beneath (EF 92) and 10 m from the fissure (EF 96) and beneath Grayton Lake (GL 2).

where V_p and V_m are the fractional volumes of water moving preferentially or in the matrix water, respectively, and sum to 1, and C_p , $^{36}\text{Cl}/C_p$, C_m , and $^{36}\text{Cl}/C_m$ refer to concentrations or ratios in water moving preferentially or in the matrix, respectively [Liu *et al.*, 1995]. The resultant $^{36}\text{Cl}/\text{Cl}$ ratios in a mixture of water moving preferentially and through the matrix were estimated by mixing 10% preferentially moving water with a bomb-pulse $^{36}\text{Cl}/\text{Cl}$ ratio of 5000×10^{-15} and Cl concentrations of 1, 10, and 100 g m^{-3} with 90% matrix water with a prebomb $^{36}\text{Cl}/\text{Cl}$ ratio of 500×10^{-15} and Cl concentrations ranging from 0.1 to $10,000 \text{ g m}^{-3}$ (Figure 12). Results indicate that the contribution of bomb-pulse $^{36}\text{Cl}/\text{Cl}$ in preferentially moving water is damped when Cl concentrations in the matrix exceed 10 to 100 g m^{-3} , as is found beneath the playa and fissure. Therefore $^{36}\text{Cl}/\text{Cl}$ ratios cannot be used to evaluate preferential flow when Cl concentrations in the matrix exceed 10 to 100 g m^{-3} . The $^{36}\text{Cl}/\text{Cl}$ ratios in the mixture decrease sharply as the Cl concentrations in the matrix increase. Uncer-

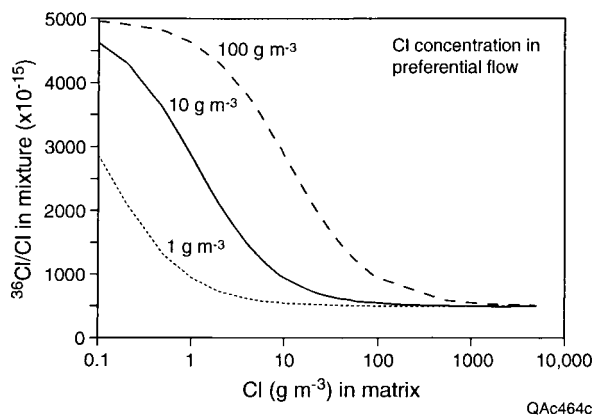


Figure 12. Damping of $^{36}\text{Cl}/\text{Cl}$ ratios in preferentially moving water (10% by volume, initial $^{36}\text{Cl}/\text{Cl}$ ratio 5000×10^{-15} , and Cl concentrations 1, 10, and 100 g m^{-3}) as a result of mixing with matrix water (90% by volume, $^{36}\text{Cl}/\text{Cl}$ ratio 500×10^{-15} , and Cl concentration 0.1 to $10,000 \text{ g m}^{-3}$).

tainties in $^{36}\text{Cl}/\text{Cl}$ ratios in preferentially moving water are not critical because $^{36}\text{Cl}/\text{Cl}$ ratios in the mixture are not very sensitive to these. Variations in the proportion of water moving preferentially from 1 to 30% resulted in only as much as 3% variation in the $^{36}\text{Cl}/\text{Cl}$ ratio of the mixture. In this arid setting (i.e., with high Cl concentrations), bomb-pulse ^3H is not as affected by mixing as are $^{36}\text{Cl}/\text{Cl}$ ratios because the short half-life of ^3H results in ^3H -free matrix water. For example, mixing 10% preferentially moving water that has bomb-pulse ^3H (estimated 100 TU) with 90% matrix water that has no ^3H results in 10 TU in the mixture. The absence of bomb-pulse $^{36}\text{Cl}/\text{Cl}$ ratios beneath the fissure and playa is therefore not inconsistent with preferential flow in these settings, as indicated by the ^3H data.

4.3.4. Diffusion. The simple CMB (1) ignores diffusion; however, Cl can be transported by advection and diffusion as shown by the following steady state equation:

$$J_{\text{Cl}} = \pm q_w c_{\text{Cluz}} - D_e \frac{\partial c_{\text{Cluz}}}{\partial z}, \quad (8)$$

where J_{Cl} is the Cl mass flux or Cl input at the surface ($M L^{-2} T^{-1}$) and D_e is the effective molecular diffusion coefficient ($L^2 T^{-1}$). The first term on the right represents the advective Cl flux (positive for upward and negative for downward), and the second term represents diffusive Cl flux. The effective molecular diffusion coefficient for Cl is calculated by multiplying the molecular diffusion coefficient in water ($0.064 \text{ m}^2 \text{ yr}^{-1}$ [Kemper, 1986]) by the volumetric water content and the tortuosity (function of water content). Bracketing values for D_e were based on tortuosity functions developed by Conca and Wright [1992] and by Millington and Quirk [1961].

The diffusive Cl flux was calculated from D_e times the Cl concentration gradient (equation (8)). In most profiles the downward diffusive Cl flux was high in the zone of steep Cl concentration gradients below the peak (Figures 1b and 13). Below this zone, diffusive Cl fluxes are much lower. Diffusive Cl fluxes are not as great where Cl concentration gradients are less steep, as in EF 91 (Figures 1b and 13b). These calculations indicate that Cl can be transported by downward diffusion

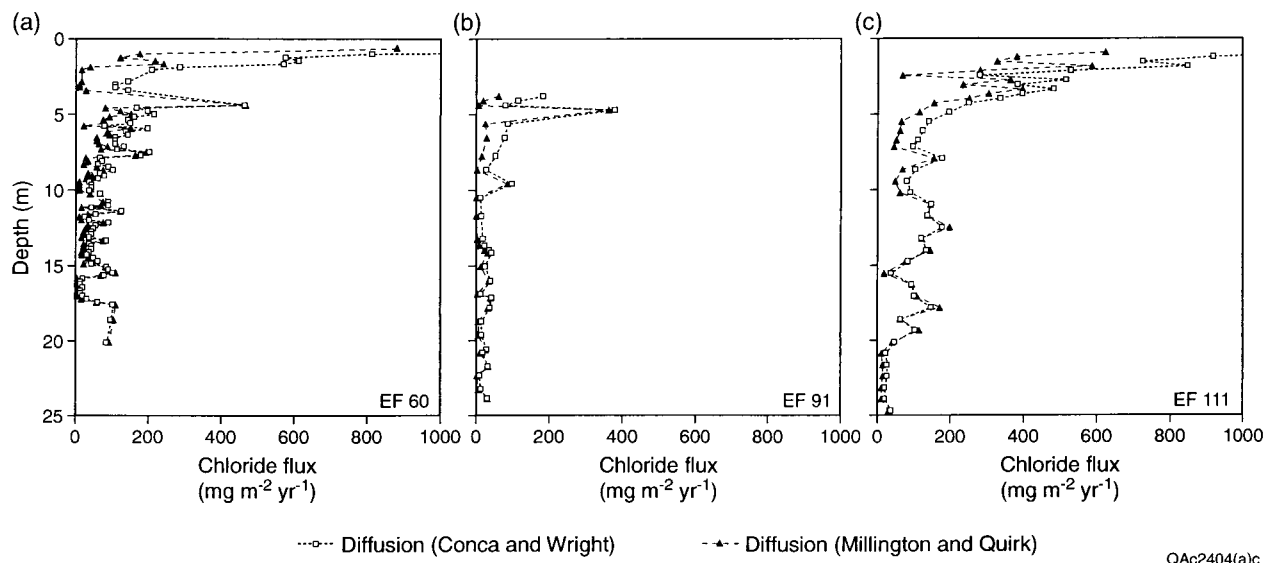


Figure 13. Diffusive Cl fluxes for (a) EF 60, (b) EF 91, and (c) EF 111 calculated using effective diffusivities from *Conca and Wright* [1992] and from *Millington and Quirk* [1961].

against an upward advective water flux; however, these diffusive Cl fluxes become negligible below the zone of steep concentration gradients. The diffusive Cl fluxes are based on current Cl profiles; however, diffusive fluxes may have been higher at depth if steep Cl concentration gradients occurred there in the past. Including diffusion at depth would reduce the CMB water flux slightly because some of the downward transport of Cl is by diffusion and is not moving with the water. Therefore CMB water fluxes that ignore diffusion represent upper bounds on actual water flux. Including diffusion should increase the age because the diffusive term would be in the denominator of (2) and would be negative because the Cl concentration gradients are negative. However, the present zone of steep Cl concentrations where diffusion is important is limited in vertical extent.

4.3.5. Anion exclusion. Because most soils outside the eolian sheet in the study area have fairly high clay content (~50%), anion exclusion may be important. Neglecting anion exclusion, as in the CMB approach, will result in overestimation of the water flux (equation (1)) because the Cl concentration in unsaturated-zone pore water will be underestimated, and Cl moves faster than water because it is restricted to the exclusion zone [Slavich and Petterson, 1993]. Underestimation of Cl concentration in pore water results from dividing the Cl concentration in the supernatant by the total water content calculated by oven drying the sample instead of the water content in the exclusion zone. In addition, the water flux needs to be corrected for more rapid transport of Cl in the exclusion zone

$$q_w = q_{wa}(1/1 - \alpha), \quad (9)$$

where q_w is the water flux ($L T^{-1}$), q_{wa} is the apparent water flux ignoring exclusion, and α is the ratio of excluded water content to total water content [Slavich and Petterson, 1993]. The two effects are multiplicative. Studies by Slavich and Petterson [1993] at a site in Australia indicate that ignoring anion exclusion in the clay-rich soil at their site resulted in overestimation of water flux from 1.25 to 1.64 times and underestimation of age by a similar amount, although a smaller

effect would be expected in the coarser-grained Eagle Flat basin sediments in this study.

4.4. Combined Effects of Uncertainties

Uncertainties in calculated CMB water fluxes and ages result from uncertainties in Cl transport processes, input, and output. Although the CMB approach assumes 1-D, downward piston flow, upward water-potential gradients and stable isotope data suggest net upward water movement in interdrainage areas. Cumulative Cl versus cumulative water plots and stable isotope data suggest probably downward water fluxes during the Pleistocene and drying since that time. Therefore water fluxes were calculated for the deeper zone (≥ 10 m), where fluxes are expected to be downward. There is no evidence of preferential flow in interdrainage areas. Although we assume that Cl is transported with water, Cl may be transported independently of water by diffusion, or it may be transported faster than the average water by anion exclusion. If water fluxes are calculated only for the deeper sections of the profiles (≥ 10 m), the effects of errors related to upward flow should be negligible. Although it is difficult to quantify the uncertainties resulting from these transport processes (diffusion and anion exclusion), they act in concert, that is, decrease the apparent CMB water flux and increase the CMB age. Ignoring all these transport processes, as is done in the simple CMB approach, results in overestimation of water flux and underestimation of age. Apparent water fluxes calculated by the CMB approach therefore constitute upper bounds and apparent ages constitute lower bounds to the extent that underlying assumptions are not met.

In interdrainage areas, for example, water fluxes calculated for the deeper sections of the profiles (≥ 10 m depth) ranged from 0.03 to 0.17 mm yr^{-1} (mean 0.06 mm yr^{-1}) using a Cl input of 87 $\text{mg m}^{-2} \text{yr}^{-1}$. Because these downward water fluxes represent older time periods, they are out of phase with current drying of the profiles. Water fluxes were calculated below the zone of steep Cl concentration gradients. Anion exclusion could reduce the apparent CMB water fluxes in clay-rich sediments. Therefore the CMB water fluxes represent an upper

bound on actual water fluxes in the interdrainage area. The low water fluxes in interdrainage settings are substantiated by thick calcic horizons (stage III) at several depths in these profiles, which imply significant evaporation of infiltrating water [Jackson *et al.*, 1993]. The estimated uncertainty in Cl input of 35% and in Cl output of $\pm 3\%$ (0.5 to 10%) results in $\pm 38\%$ uncertainty in calculated CMB water flux at depths ≥ 10 m (Table 1). The uncertainties in Cl input and output are considered error bars on the upper bounding estimate that results from uncertainties in transport mechanisms.

Residence times of Cl in interdrainage areas ranged from 27,515 years for EF 91 to 136,000 years for EF 111 at 25-m depth. Uncertainties in transport mechanisms, such as diffusion and anion exclusion, result in the calculated CMB residence times being lower bounds on actual residence times. All these transport processes act in concert and increase the residence time of Cl. The general correspondence of the CMB ages and ages based on radioactive decay of ^{36}Cl indicates that overestimation of water residence time by the CMB approach is probably not greater than a factor of 2 or 3. The estimated uncertainty in Cl input of $\pm 35\%$ and Cl output of $\pm 3\%$ (0.5 to 10%) results in asymmetric errors (-24 to 56%) in the CMB calculated average residence time because of the inverse relationship between residence time and chloride output (Table 1).

In drainage areas or areas where surface water ponds, the CMB approach is much more difficult to apply because of (1) uncertainties in transport mechanisms (preferential flow), (2) large uncertainties in Cl input because of Cl in run-on, (3) reduced sensitivity of Cl to changes in water flux at low Cl concentrations, and (4) analytical uncertainty in Cl concentration measurements at low concentrations.

Preferential flow, as shown by ^3H data beneath the fissure and playa, should affect CMB water flux. Because the CMB approach does not account for preferential flow, it therefore underestimates water flux in these areas. However, uncertainty in Cl input or run-on may be much greater than that of preferential flow. Cl provided in run-on is estimated to result in about an order of magnitude uncertainty in Cl input. Mean Cl concentrations ranged from 92 g m^{-3} beneath Blanca Draw (EF 110) to 21 g m^{-3} beneath the fissure (top 7.5 m of EF 120). Downward water fluxes calculated by the CMB approach ranged from 0.2 to 20 mm yr^{-1} (EF 110) beneath Blanca Draw and from 0 to 25 mm yr^{-1} (EF 120) beneath the fissure. Ignoring preferential flow and run-on results in underestimation of water flux by about an order of magnitude. Average uncertainties in water flux resulting from uncertainties in Cl output or analytical uncertainties in Cl measurements ($\pm 12\%$) ranged from -11 to 13% in drainage and fissure profiles (Figure 6a and Table 1) (Appendix B). Uncertainties in water flux can be as high as 479% . Analytical uncertainties increase as Cl concentrations decrease.

The process of estimating uncertainties in water flux and age from environmental tracers described in this study is generally applicable to systems characterized by porous media in semi-arid and arid regions. Chloride profiles described in this study are similar to those in other desert basins [Tyler *et al.*, 1996; Prudic, 1994]; therefore the findings from this study should be generally applicable to those regions. Uncertainties in Cl input and output should be similar to those used in this study also. However, specific analysis of uncertainties should be conducted at each site using both soil physics and a variety of environmental tracers as shown in this study. Although we have not specifically addressed fractured media in this work,

fractured systems would be somewhat similar to the playa setting where desiccation cracks are found in the clay sediments. Preferential flow is an important issue in fractured media and should result in underestimation of water flux by the CMB approach. Analysis of Cl in perched aquifers or shallow water tables would provide a much better integrated estimate of water flux in fractured media.

4.5. Example Application of Uncertainty Analysis

In interdrainage areas, for example, using data from the EF 111 profile, the average water flux at depths ≥ 10 m is 0.04 mm yr^{-1} , and the CMB age at the base of the profile (25 m) is 136,000 years. Uncertainties in transport mechanisms result in these estimates of water flux being upper bounds on actual water fluxes and estimates of age being lower bounds on actual ages. Uncertainties in these bounding estimates result from uncertainty in the Cl input ($\sim \pm 35\%$), which results in $\pm 35\%$ uncertainty in water flux and -26 to 54% uncertainty in age, and from analytical uncertainties in Cl measurements, which result in $\pm 3\%$ uncertainty in water flux and $\pm 2\%$ uncertainty in age. The combined effect of uncertainties in Cl input and Cl output measurements results in $\pm 38\%$ uncertainty in water flux (0.02 mm yr^{-1}) and -24 to 56% uncertainty in age (103,360 to 212,160 years).

In drainage areas, for example, using data from the EF 110 profile, the average water flux is $\sim 3 \text{ mm yr}^{-1}$ (0.2 to 20 mm yr^{-1}), and the CMB age at the base of the profile (26 m) is 8500 years. Preferential flow and uncertainty in Cl input from run-on (\sim order of magnitude) result in the calculated CMB water fluxes representing lower bounds, and actual water fluxes could be an order of magnitude higher. Uncertainties in Cl output from analytical uncertainties in Cl measurements in this profile are about $\pm 12\%$ and result in an uncertainty range of -11 to 13% in the lower bounding estimate of water flux. Although it is difficult or impossible to quantify all sources of uncertainty, the uncertainty analysis in this study shows that calculated water fluxes and ages based on the CMB approach can generally provide bounding estimates on actual water fluxes and ages.

5. Conclusions

The long residence times suggested by the Cl data in interdrainage areas (55,000 to 105,000 years) were generally corroborated by residence times estimated from radioactive decay of ^{36}Cl ($39,000 \pm 13,000$ to $59,000 \pm 14,400$ years). The various sources of uncertainty with the use of the CMB approach include uncertainties in transport processes, Cl input, and Cl output. Uncertainties in transport processes were evaluated using physical data and information from other tracers. In interdrainage areas, water-potential and stable isotope data indicate net upward water movement. Cl and stable isotope data suggest that this drying trend may have persisted through the Holocene and that water movement was probably downward in the Pleistocene. Although Cl is generally assumed to be transported with water, diffusion and anion exclusion could result in faster transport of Cl relative to water. Diffusion is important in the zone of steep concentration gradients near the surface. Because of upward flow and diffusion, the CMB approach was applied only to older, deeper sections of the profiles (≥ 10 m) to calculate water flux. By ignoring these processes, such as diffusion and anion exclusion, the CMB approach provides an upper bound on actual water flux and a

lower bound on actual age because these processes decrease water flux and increase age. Water fluxes estimated for deeper sections of profiles (≥ 10 m) in interdrainage areas are low (0.03 to 0.2 mm yr $^{-1}$, mean 0.06 mm yr $^{-1}$). Error bars on these bounding estimates were evaluated on the basis of uncertainty in Cl input ($\sim \pm 35\%$) and in Cl output ($\pm 3\%$) that result in $\pm 38\%$ uncertainty in water flux and -24 to 56% uncertainty in water age in interdrainage areas.

In drainage areas the CMB approach is much more difficult to apply because of (1) uncertainties in transport mechanisms (preferential flow as shown by ^3H), (2) large uncertainties in Cl input because of Cl in run-on (order of magnitude uncertainty), (3) reduced sensitivity of Cl to changes in water flux at low Cl concentrations, and (4) analytical uncertainty in Cl concentration measurements at these low levels. The CMB water fluxes therefore constitute a lower bound on the actual water flux, and the CMB ages constitute an upper bound on the actual age. Calculated water fluxes ranged from 0.02 to 25 mm yr $^{-1}$ (mean 3 mm yr $^{-1}$). Inclusion of Cl in run on would increase these water flux estimates by about an order of magnitude. Error bars on this lower bounding estimate (-11 to 13%) result from uncertainties in Cl output (mean $\pm 12\%$).

The results of this study have important implications for waste disposal in arid regions characterized by porous media because they suggest that water fluxes estimated using the CMB approach are conservatively high in interdrainage areas where disposal facilities are generally located. Comprehensive uncertainty analysis requires information from other tracer and physical techniques to provide greater confidence than that provided by a single tracer.

Appendix A

Uncertainties in age (1σ) calculated from radioactive decay of ^{36}Cl (equation (3)) were evaluated according to the following equations [Bevington and Robinson, 1992, pp. 42–43]:

$$\sigma_t = \left[\left(\frac{\partial t}{\partial R} \right)^2 \sigma_R^2 + \left(\frac{\partial t}{\partial R_0} \right)^2 \sigma_{R_0}^2 + \left(\frac{\partial t}{\partial R_{se}} \right)^2 \sigma_{R_{se}}^2 \right]^{0.5} \quad (\text{A1})$$

$$\sigma_t = \left\{ \left(\frac{\sigma_R}{\lambda_{36}(R - R_{se})} \right)^2 + \left(\frac{\sigma_{R_0}}{\lambda_{36}(R_0 - R_{se})} \right)^2 + \left[\frac{1}{\lambda_{36}} \left(\frac{1}{R_0 - R_{se}} - \frac{1}{R - R_{se}} \right) \right]^2 \sigma_{R_{se}}^2 \right\}^{0.5}, \quad (\text{A2})$$

where σ_t is the uncertainty in the age, λ_{36} is the decay constant for ^{36}Cl (2.30×10^{-6} yr $^{-1}$), R is the measured $^{36}\text{Cl}/\text{Cl}$ ratio, R_{se} is the secular equilibrium $^{36}\text{Cl}/\text{Cl}$ ratio ($\sim 10 \times 10^{-15}$) [Bentley *et al.*, 1986], R_0 is the initial $^{36}\text{Cl}/\text{Cl}$ ratio (e.g., 491×10^{-15} at 10.7 m depth for the EF 60 profile), σ_R is the uncertainty in the $^{36}\text{Cl}/\text{Cl}$ ratio measurements, $\sigma_{R_{se}}$ is the estimated uncertainty in the secular equilibrium $^{36}\text{Cl}/\text{Cl}$ ratio (0.5×10^{-15}), and σ_{R_0} is the measured uncertainty in the initial $^{36}\text{Cl}/\text{Cl}$ ratio (e.g., 11×10^{-15} at 10.7 m depth for the EF 60 profile) (J. T. Fabryka-Martin, personal communication, 1998).

Appendix B

Uncertainty in water flux (q) resulting from uncertainty in Cl concentrations ($\varepsilon_{c_{\text{Cluz}}}$) in unsaturated zone pore water was calculated from (1) as follows:

$$q = \frac{J_{\text{Cl}}}{c_{\text{Cluz}}} = \frac{k}{c_{\text{Cluz}}} \quad q^+ = \frac{k}{(1 + \varepsilon_{c_{\text{Cluz}}})c_{\text{Cluz}}} \quad (\text{B1})$$

$$q^- = \frac{k}{(1 - \varepsilon_{c_{\text{Cluz}}})c_{\text{Cluz}}}$$

$$\varepsilon_{fq^+} = \frac{q^+ - q}{q} = \frac{\frac{k}{(1 + \varepsilon_{c_{\text{Cluz}}})c_{\text{Cluz}}} - \frac{k}{c_{\text{Cluz}}}}{\frac{k}{c_{\text{Cluz}}}} = \frac{1}{1 + \varepsilon_{c_{\text{Cluz}}}} - 1 \quad (\text{B2})$$

$$\varepsilon_{fq^-} = \frac{q - q^-}{q} = \frac{1}{1 - \varepsilon_{c_{\text{Cluz}}}} - 1, \quad (\text{B3})$$

where J_{Cl} is the Cl input (treated as constant (k)), q^+ (q^-) is the q resulting from an increase (decrease) in c_{Cluz} by the error in c_{Cluz} ($\varepsilon_{c_{\text{Cluz}}}$). Fractional uncertainty in age resulting from uncertainty in Cl input was calculated from (2) as follows:

$$t = \frac{\int_0^z \theta c_{\text{Cluz}} dz}{J_{\text{Cl}}} = \frac{k}{J_{\text{Cl}}} \quad t^+ = \frac{k}{(1 + \varepsilon_{J_{\text{Cl}}})J_{\text{Cl}}} \quad (\text{B4})$$

$$t^- = \frac{k}{(1 - \varepsilon)J_{\text{Cl}}}$$

$$\varepsilon_{ft^+} = \frac{t^+ - t}{t} = \frac{\frac{k}{(1 + \varepsilon_{J_{\text{Cl}}})J_{\text{Cl}}} - \frac{k}{J_{\text{Cl}}}}{\frac{k}{J_{\text{Cl}}}} = \frac{1}{1 + \varepsilon_{J_{\text{Cl}}}} - 1 \quad (\text{B5})$$

$$\varepsilon_{ft^-} = \frac{t - t^-}{t} = \frac{1}{1 - \varepsilon_{J_{\text{Cl}}}} - 1. \quad (\text{B6})$$

Because $\varepsilon_{J_{\text{Cl}}}$ is 0.35,

$$\varepsilon_{ft^+} = \frac{1}{1 + \varepsilon_{J_{\text{Cl}}}} - 1 = \frac{1}{1 + 0.35} - 1 = -0.26 \quad (\text{B7})$$

$$\varepsilon_{ft^-} = \frac{1}{1 - \varepsilon_{J_{\text{Cl}}}} - 1 = \frac{1}{1 - 0.35} - 1 = 0.54.$$

Uncertainty in age resulting from uncertainty in Cl concentrations in pore water was calculated from (2) as follows:

$$\varepsilon_{ft_i} = \frac{\varepsilon_{t_i}}{t_i} = \frac{\varepsilon_{ft_{i-1}} + \Delta t_i \frac{\varepsilon_{c_{\text{Cluz}}}}{c_{\text{Cluz}}}}{t_{i-1} + \Delta t_i} \quad (\text{B8})$$

$$\frac{\varepsilon_{t_i}}{t_i} = \frac{\varepsilon_{c_{\text{Cluz}}}}{c_{\text{Cluz}}} \quad i = 1, \quad t_{i-1} = 0, \quad \varepsilon_{t_{i-1}} = 0. \quad (\text{B9})$$

Appendix C

The isotopic data were used to calculate subsurface evaporation rates in the interdrainage areas (1) from the position of the isotopic peak and (2) from “the decay length method in the liquid transport region” [Barnes and Allison, 1983, 1988]. The isotopic maximum (point 1) in the profiles was used to estimate the evaporation rate as follows:

$$E = N_{\text{sat}} D^{v*} (1 - h_a) / \rho z_{ef}, \quad (\text{C1})$$

where E is the evaporation rate ($L T^{-1}$), N_{sat} is water vapor concentration at saturation ($M L^{-3}$), D^{v*} is the effective vapor diffusivity ($L^2 T^{-1}$), h_a is the relative humidity of the atmosphere (mean annual ~ 0.5), ρ_l is the liquid water density ($M L^{-3}$), and z_{ef} is the depth of the evaporation front [Barnes and Allison, 1983]. The evaporation rate was also estimated from the decay length (point 2):

$$\frac{\delta_i - \delta_i^{\text{res}}}{\delta_i^{\text{ef}} - \delta_i^{\text{res}}} = \exp(-f(z)/\hat{z}_i), \quad (C2)$$

where δ refers to the isotopic ratio relative to VSMOW, δ_i is the δ value at each depth, δ_i^{res} is the δ value at the base of the profile (reservoir), δ_i^{ef} is the δ value at the evaporation front, $f(z)$ is a depth function [Barnes and Allison, 1984], and \hat{z}_i is the decay length (L , the isotopic value at the evaporation front divided by e) [Barnes and Allison, 1983]. The decay length (\hat{z}_i) is calculated from this equation and is used to estimate the evaporation rate:

$$E = D_{l+v}^* / \hat{z}_i, \quad (C3)$$

where D_{l+v}^* is the combined effective liquid and vapor diffusion coefficients ($L^2 T^{-1}$).

Acknowledgments. This research was funded by the Texas Low-Level Radioactive Waste Disposal Authority. Jinhua Liang assisted with data reduction. The author is grateful for the chemical analyses of rainwater conducted at Los Alamos National Laboratory by Laura Wolfsberg under the direction of June Fabryka-Martin. The author greatly appreciates helpful discussions with Jenny Chapman and Scott Tyler (Desert Research Institute), June Fabryka-Martin (Los Alamos National Laboratory), Glendon Gee (Pacific Northwest National Laboratory), Jim Jennings (Bureau of Economic Geology), Mitch Plummer and Fred Phillips (New Mexico Tech), and an anonymous reviewer. The author would like to acknowledge reviews by Peter Cook (CSIRO), June Fabryka-Martin (LANL), Fred Phillips (New Mexico Tech), and Eric Sonnenthal (Lawrence Berkeley National Laboratory), whose comments greatly improved the quality of the manuscript. Publication is authorized by the Director, Bureau of Economic Geology, University of Texas at Austin.

References

- Allison, G. B., The relationship between ^{18}O and deuterium in water in sand columns undergoing evaporation, *J. Hydrol.*, **55**, 163–169, 1982.
- Allison, G. B., and M. W. Hughes, The use of environmental chloride and tritium to estimate total recharge to an unconfined aquifer, *Aust. J. Soil Res.*, **16**, 181–195, 1978.
- Allison, G. B., G. W. Gee, and S. W. Tyler, Vadose zone techniques for estimating groundwater recharge in arid and semiarid regions, *Soil Sci. Soc. Am. J.*, **58**, 6–14, 1994.
- Barnes, C. J., and G. B. Allison, The distribution of deuterium and oxygen-18 in dry soils, I, Theory, *J. Hydrol.*, **60**, 141–156, 1983.
- Barnes, C. J., and G. B. Allison, Distribution of deuterium and oxygen-18 in dry soils, 3, Theory for nonisothermal water movement, *J. Hydrol.*, **74**, 119–135, 1984.
- Barnes, C. J., and G. B. Allison, Tracing of water movement in the unsaturated zone using stable isotopes of hydrogen and oxygen, *J. Hydrol.*, **100**, 143–176, 1988.
- Bentley, H. W., F. M. Phillips, and S. N. Davis, ^{36}Cl in the terrestrial environment, in *Handbook of Environmental Isotope Geochemistry*, vol. 2b, edited by P. Fritz and J.-C. Fontes, pp. 422–475, Elsevier Sci., New York, 1986.
- Bevington, P. R., and D. K. Robinson, *Data Reduction and Error Analysis for the Physical Sciences*, 328 pp., McGraw-Hill, New York, 1992.
- Conca, J. L., and J. V. Wright, Diffusion and flow in gravel, soil, and whole rock, *Appl. Hydrogeol.*, **1**, 5–24, 1992.
- Cook, P. G., W. M. Edmunds, and C. B. Gaye, Estimating paleorecharge and paleoclimate from unsaturated zone profiles, *Water Resour. Res.*, **28**, 2721–2731, 1992.
- Davis, S. N., D. O. Whittemore, and J. Fabryka-Martin, Uses of chloride/bromide ratios in studies of potable water, *Ground Water*, **36**, 338–350, 1998.
- Elmore, D., B. R. Fulton, M. R. Clover, J. R. Marsden, H. E. Gove, H. Naylor, K. H. Purser, L. R. Kilius, R. P. Beukens, and A. E. Litherland, Analysis of ^{36}Cl in environmental water samples using an electrostatic accelerator, *Nature*, **227**, 22–25, 1979.
- Elmore, D., N. J. Conard, P. W. Kubik, and J. Fabryka-Martin, Computer controlled isotope ratio measurements and data analysis, *Nucl. Instrum. Methods Phys. Res.*, **B5**, 233–237, 1984.
- Fabryka-Martin, J. T., Production of radionuclides in the Earth and their hydrogeologic significance, with emphasis on chlorine-36 and iodine-129, Ph.D. dissertation, 400 pp., Univ. of Ariz., Tucson, 1988.
- Fabryka-Martin, J. T., S. J. Wightman, W. J. Murphy, M. P. Wickham, M. W. Caffee, G. J. Nimz, J. R. Southon, and P. Sharma, Distribution of chlorine-36 in the unsaturated zone at Yucca Mountain: An indicator of fast transport paths, in *Focus '93: Site Characterization and Model Validation*, pp. 58–68, Am. Nucl. Soc., La Grange Park, Ill., 1993.
- Fabryka-Martin, J. T., A. V. Wolfsberg, S. S. Levy, J. L. Roach, S. T. Winters, L. E. Wolfsberg, D. Elmore, and P. Sharma, Distribution of fast hydrologic paths in the unsaturated zone at Yucca Mountain, in *Proceedings of the 8th Annual International High-Level Radioactive Waste Management Conference*, pp. 93–96, Am. Nucl. Soc., La Grange Park, Ill., 1998.
- Ginn, T. R., and E. M. Murphy, A transient flux model for convective infiltration: Forward and inverse solutions for chloride mass balance studies, *Water Resour. Res.*, **33**, 2065–2079, 1997.
- Guyodo, Y., and J.-P. Valet, Relative variations in geomagnetic intensity from sedimentary records: The past 200,000 years, *Earth Planet. Sci. Lett.*, **143**, 23–26, 1996.
- Hainsworth, L. J., A. C. Mignerey, G. R. Helz, P. Sharma, and P. W. Kubik, Modern chlorine-36 deposition in southern Maryland, U.S.A., *Nucl. Instrum. Methods Phys. Res.*, **B92**, 345–359, 1994.
- Holser, W. T., Mineralogy of evaporites, in *Marine Minerals*, vol. 6, edited by R. G. Burns, pp. 211–294, Mineral. Soc. of Am., Washington, D. C., 1979.
- Ingraham, N. L., and C. Shadel, A comparison of the toluene distillation and vacuum/heat methods for extracting soil water for stable isotopic analysis, *J. Hydrol.*, **140**, 371–387, 1992.
- International Atomic Energy Agency, Isotope techniques in the hydrogeological assessment of potential sites for the disposal of high-level radioactive wastes, *IAEA Tech. Rep. Ser. 228*, chap. 7, pp. 57–61, Vienna, 1983.
- Jackson, M. L. W., R. P. Langford, and M. J. Whitelaw, Basin-fill stratigraphy, quaternary history, and paleomagnetism of the Eagle Flat study area, southern Hudspeth County, Texas, 137 pp., final contract report, Bur. of Econ. Geol., Univ. of Tex. at Austin, 1993.
- Kemper, W. D., Solute diffusivity, in *Methods of Soil Analysis*, Part 2, *Chemical and Microbiological Methods*, *Agron. Monogr.*, vol. 9, edited by A. Klute, pp. 1007–1024, Am. Soc. of Agron., Madison, Wis., 1986.
- Knies, D. L., ^7Be , ^{10}Be , and ^{36}Cl in Precipitation: Ph.D. dissertation, Purdue Univ., 114 pp., West Lafayette, Indiana, 1995.
- Lal, D., and B. Peters, Cosmic ray produced radioactivity on the Earth, in *Handbuch der Physik 46/2*, edited by S. Kitte, pp. 551–612, Springer-Verlag, New York, 1967.
- Langford, R. P., Landscape evolution of Eagle Flat and Red Light Draw Basins, Chihuahuan Desert, south-central Trans-Pecos Texas, final contract report prepared for the Texas Low-Level Radioactive Waste Disposal Authority, 153 pp., Bur. Econ. Geol., Univ. of Tex. at Austin, 1993.
- Larkin, T. J., and G. W. Bomar, *Climatic Atlas of Texas*, map LP-192, Tex. Dep. Water Resour., Austin, Tex., 1983.
- Liu, B., J. Fabryka-Martin, A. Wolfsberg, B. Robinson, and P. Sharma, Significance of apparent discrepancies in water ages derived from atmospheric radionuclides at Yucca Mountain, Nevada, in *Water Resources at Risk*, edited by W. R. Hotchkiss, J. S. Downey, E. D. Gutentag, and J. E. Moore, pp. NH52–NH62, Am. Inst. of Hydrol., Minneapolis, Minn., 1995.
- Mattick, J. L., T. A. Duval, and F. M. Phillips, Quantification of groundwater recharge rates in New Mexico using bomb ^{36}Cl , bomb ^3H and chloride as soil-water tracers, *Rep. 220*, 184 pp., N. M. Water Resour. Res. Inst., Las Cruces, 1987.

- Millington, R. J., and J. P. Quirk, Permeability of porous solids, *Trans. Faraday Soc.*, 57(7), 1200–1207, 1961.
- Murphy, E. M., T. R. Ginn, and J. L. Phillips, Geochemical estimates of recharge in the Pasco basin: Evaluation of the chloride mass balance technique, *Water Resour. Res.*, 32, 2853–2868, 1996.
- Nativ, R., E. Adar, O. Dahan, and M. Geyh, Water recharge and solute transport through the vadose zone of fractured chalk under desert conditions, *Water Resour. Res.*, 31, 253–261, 1995.
- Peck, A. J., C. D. Johnston, and D. R. Williamson, Analyses of solute distributions in deeply weathered soils, *Agric. Water Manage.*, 4, 83–102, 1981.
- Phillips, F. M., Environmental tracers for water movement in desert soils of the American southwest, *Soil Sci. Soc. Am. J.*, 58, 14–24, 1994.
- Phillips, F. M., Chlorine-36 in subsurface hydrology, in *Environmental Tracers in Subsurface Hydrology*, edited by P. G. Cook and A. L. Herczeg, Kluwer Acad., Norwell, Mass., 1999.
- Phillips, F. M., J. L. Mattick, and T. A. Duval, Chlorine-36 and tritium from nuclear weapons fallout as tracers for long-term liquid movement in desert soils, *Water Resour. Res.*, 24, 1877–1891, 1988.
- Phillips, F. M., D. B. Rogers, S. J. Dreiss, N. O. Jannik, and D. Elmore, Chlorine 36 in Great Basin waters: Revisited, *Water Resour. Res.*, 31, 3195–3204, 1995.
- Plummer, M. A., F. M. Phillips, J. Fabryka-Martin, H. J. Turin, P. E. Wigand, and P. Sharma, Chlorine-36 in fossil rat urine: An archive of cosmogenic nuclide deposition during the past 40,000 years, *Science*, 277, 538–541, 1997.
- Prudic, D. E., Estimates of percolation rates and ages of water in unsaturated sediments at two Mojave Desert sites, California-Nevada, *U.S. Geol. Surv. Water Resour. Invest. Rep.*, 94-4160, 19 pp., 1994.
- Reheis, M. C., and R. Kihl, Dust deposition in southern Nevada and California, 1984–1989: Relations to climate, source area, and source lithology, *J. Geophys. Res.*, 100, 8893–8918, 1995.
- Scanlon, B. R., Evaluation of liquid and vapor flow in desert soils based on chlorine-36 and tritium tracers and nonisothermal flow simulations, *Water Resour. Res.*, 28, 285–297, 1992.
- Scanlon, B. R., and R. S. Goldsmith, Field study of spatial variability in unsaturated flow beneath and adjacent to playas, *Water Resour. Res.*, 33, 2239–2252, 1997.
- Scanlon, B. R., R. S. Goldsmith, and J. P. Paine, Analysis of unsaturated flow beneath fissures in the Chihuahuan Desert, Texas, USA, *J. Hydrol.*, 203, 58–78, 1997a.
- Scanlon, B. R., S. W. Tyler, and P. J. Wierenga, Hydrologic issues in arid systems and implications for contaminant transport, *Rev. Geophys.*, 35(4), 461–490, 1997b.
- Scanlon, B. R., R. S. Goldsmith, and R. S. Langford, *Geomorphic Controls on Subsurface Flow in an Arid Setting: Case Study in the Chihuahuan Desert, Texas*, investigation report, Bur. of Econ. Geol., Univ. of Tex. at Austin, 1999a.
- Scanlon, B. R., R. P. Langford, and R. S. Goldsmith, Relationship between geomorphic settings and unsaturated flow in an arid setting, *Water Resour. Res.*, 35, 983–999, 1999b.
- Slavich, P. G., and G. H. Petterson, Anion exclusion effects on estimates of soil chloride and deep percolation, *Aust. J. Soil Res.*, 31, 455–463, 1993.
- Taylor, J. R., *An Introduction to Error Analysis, The Studies of Uncertainties in Physical Measurements*, 270 pp., Oxford Univ. Press, New York, 1982.
- Tyler, S. W., J. B. Chapman, S. H. Conrad, D. P. Hammermeister, D. O. Blout, J. J. Miller, M. J. Sully, and J. M. Ginanni, Soil-water flux in the southern Great Basin, United States: Temporal and spatial variations over the last 120,000 years, *Water Resour. Res.*, 32, 1481–1499, 1996.
- Wood, W. W., and W. E. Sanford, Chemical and isotopic methods for quantifying ground-water recharge in a regional, semiarid environment, *Ground Water*, 33, 458–468, 1995a.
- Wood, W. W., and W. E. Sanford, Eolian transport, saline lake basins, and groundwater solutes, *Water Resour. Res.*, 31, 3121–3129, 1995b.
- Yang, I. C., G. W. Rattray, and P. Yu, Interpretations of chemical and isotopic data from boreholes in the unsaturated zone at Yucca Mountain, Nevada, in *U.S. Geol. Surv. Water Resour. Invest. Rep.*, WRIR 96-4058, 1996.

B. Scanlon, Bureau of Economic Geology, University of Texas at Austin, J. J. Pickle Research Campus, Building 130, 10100 Burnet Road, Austin, TX 78713-8924. (Bridget.Scanlon@beg.utexas.edu)

(Received January 13, 1999; revised July 1, 1999; accepted July 27, 1999.)

